Spatio-spectral characterization of ultrashort laser pulses with a birefringent delay line

Spencer Jolly, Olivier Gobert, Fabien Quéré

Research Article | Vol. 4, No. 7 / 15 July 2021 / OSA Continuum 2044

Spatio-spectral characterization of ultrashort laser pulses with a birefringent delay line

SPENCER W. JOLLY,[1,2,3] OLIVIER GOBERT,[1,4] AND FABIEN QUÉRÉ[1,5]

[1] *LIDYL, CEA, CNRS, Université Paris-Saclay, CEA Saclay, 91191, Gif-sur-Yvette, France*
[2] *Currently Brussels Photonics (B-PHOT), Dept. of Applied Physics and Photonics, Vrije Universiteit Brussel, Pleinlaan 2, 1050 Brussels, Belgium*
[3] *spencer.jolly@vub.be*
[4] *olivier.gobert@cea.fr*
[5] *fabien.quere@cea.fr*

Abstract: We utilize a birefringent delay line to perform spatially-resolved Fourier transform spectroscopy at multiple planes around the focus of an ultrashort laser pulse. Combining these measurements at multiple planes with phase-retrieval, i.e. the INSIGHT technique, allows for the determination of the three-dimensional laser field, in both amplitude and phase, lacking only the knowledge of a spatially-uniform spectral phase. We use the device to simultaneously measure two low-order spatio-temporal couplings resulting from a misaligned chromatic lens doublet. Besides being a new implementation of spatio-spectral characterization of ultrashort pulses, this technique allows for more accuracy and stability in spatio-spectral characterization and a push to shorter wavelengths, and may ultimately enable sparse measurements.

1. Introduction

Spatio-temporal couplings (STCs) and spatio-spectral couplings are generally aberrations on ultrashort laser pulses that lead to the space and time or space and frequency descriptions of the laser field to be inseparable [1]. There are many techniques for spatio-temporal characterization [2,3], which often involve spatio-spectral characterization followed by a spectral phase measurement at a single transverse position, allowing for calculating the spatio-temporal field via the Fourier-transform. One of these techniques is the INSIGHT technique for spatio-spectral characterization near the focus of an ultrashort beam [4]. With INSIGHT, Fourier-transform spectroscopy (FTS) is used at the focus, resolved on a CCD camera, to measure the spatio-spectral amplitude profile. The measurement of the spatially-resolved spectrum (equivalently the spectrally-resolved beam profile) is repeated at multiple planes around the focus which then allows for the use of phase-retrieval algorithms to calculate the spatio-spectral phase, completing the knowledge of the full 3D complex field. INSIGHT was previously implemented using a Michelson interferometer and required sub-cycle delay accuracy. The challenge of reaching sub-cycle delay steps required using expensive piezo-electric translation stages, which still have inherent noise and instability with such small steps. We present here a device which is a new implementation of the INSIGHT technique using an interferometer based on a delay line composed of birefringent prisms [5], which is essentially a modified Babinet-Soleil retarder.

An interferometer based on a birefringent delay line has been used for stable two-dimensional Fourier-transform spectroscopy in the infrared [6,7], referred to as the TWINS device (Translating-Wedge-Based Identical Pulses eNcoding System) [8]. Because it has very accurate and stable delay-stepping, TWINS has been extended to two-dimensional spectroscopy in the visible range [9] and demonstrated successful application to hyperspectral imaging (also in the visible range) [10,11], available now in a range of industrial devices [12]. Such a delay line has even been used for high-harmonic generation studies [13,14].

#430432 https://doi.org/10.1364/OSAC.430432
Journal © 2021 Received 30 Apr 2021; revised 31 May 2021; accepted 19 Jun 2021; published 9 Jul 2021

OSA CONTINUUM

In our case we aim to simplify and improve spatio-temporal characterization of ultrashort laser pulses using FTS by eliminating expensive piezoelectric stages and reducing the noise in the calculated spectrum associated with error in the delay steps [15]. Because we use the INSIGHT technique for measuring the ultrashort pulses combined with the TWINS technique for generating the necessary delay, we refer to our technique as TWINS-INSIGHT. In this work we show a first demonstration of this device for measuring common spatio-temporal couplings.

2. Experimental implementation

A schematic of the TWINS-INSIGHT apparatus is shown in Fig. 1. The INSIGHT technique involves measuring the spatio-spectral amplitude via FTS at three planes around the focus, and the TWINS technique is used to generate the precise delay steps between the two beam replicas. In general the entire setup can be translated in order to allow for measurements at the three distinct planes. After measuring the three spatio-spectral amplitude profiles, the spatio-spectral phase at the focus is calculated using phase-retrieval algorithms [4]. Using the reconstructed complex spatio-spectral field at the focus, the field can be numerically propagated to any plane of interest.

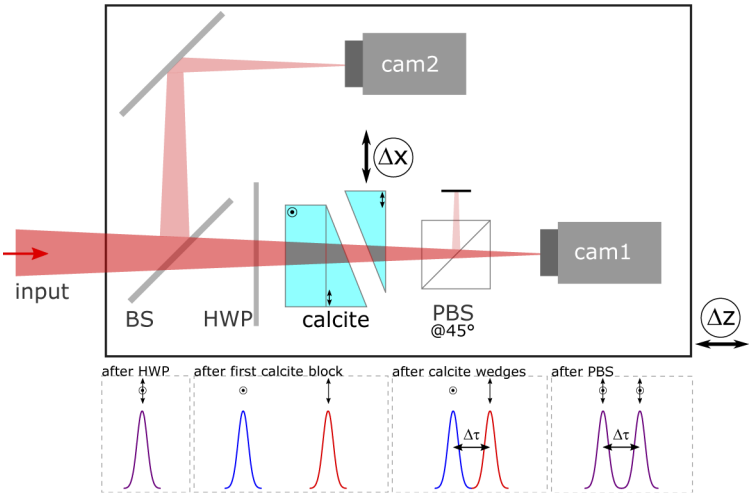

Fig. 1. A schematic of the TWINS-INSIGHT setup. The converging laser beam is split with a beamsplitter (BS), where the main arm goes through the TWINS section, which produces two replicas that then interfere on the signal camera (cam1). The split beam in the other arm goes to the auxiliary camera (cam2) to measure the shot-to-shot pointing fluctuations and correct for them in post-processing. Within the TWINS arm the polarization is rotated by a half-wave plate (HWP) and the variable delay is generated by a calcite block and a pair of calcite wedges ($\Delta\tau \propto \Delta x$). Then, finally, a polarizing beamsplitter projects the delayed pulse copies onto the same axis. The polarization states at different points in the setup are visualized at the bottom of the figure. To move to different measurement planes, necessary for the INSIGHT method, the entire setup can be translated (Δz, bottom right arrow).

In our apparatus the converging input beam is split into two arms where one arm provides a reference for shot-to-shot pointing fluctuations and the other arm is the interference signal. The polarization of the converging beam in the signal arm is rotated by a half-wave plate to have 45 deg. linear polarization. Then with this polarization, the beam propagates through the birefringent calcite optics, which produce a tunable delay between the 0 deg. and 90 deg. orthogonal polarizations. The first calcite block with a vertical optic axis produces an initial temporal offset between the two polarizations, and then the set of wedges with a horizontal optic

OSA CONTINUUM

axis compensates for that initial offset. The second wedge in the pair is translated perpendicular to the beam axis to effectively tune the total thickness of calcite with a horizontal optic axis ($\Delta\tau \propto \Delta x$). If the second wedge is precisely aligned with the first wedge ($\Delta x = 0$) then the delay is zero. After generating this tunable delay a polarizing beamsplitter oriented at 45 deg. projects both polarizations onto the same axis with their relative delay remaining, allowing for inteference on the signal camera. Finally, as mentioned earlier, the entire setup can be translated to measure at the planes out of focus to have the information necessary to retrieve the spatio-spectral phase. This translation could also be done with the signal camera only, or the interfering beams could be further split on to other cameras outside of focus, but we preferred to leave the setup as simple as possible for this demonstration.

Our design for the TWINS section of TWINS-INSIGHT is composed of wedges made from calcite with a φ =5 deg. wedge angle. The delay step τ_{step} possible with a certain step of the wedge perpendicular to the beam x_{step} is as follows

$$x_{\text{step}} = \frac{c\tau_{\text{step}}}{\Delta n_g \tan(\varphi)}. \tag{1}$$

We expect from literature values that $\Delta n_g = n_g^{(e)} - n_g^{(o)} = -0.1817$ for calcite at a wavelength of 800 nm [16], corresponding to an 18.86 μm step (with a 5 degree wedge angle) to change the relative delay by 1 fs, necessary for sub-cycle steps when characterizing a beam with an 800 nm central wavelength. This is a 126 times larger step size than needed to create 1 fs of delay in a standard retro-reflecting piezo-electric delay line (150 nm). Indeed, this is the biggest benefit of the TWINS technique, that smaller delay steps can be made with larger physical translations, and also that the absolute delay can be known with more precision. The device is also simpler to align and more robust in the presence of vibrations. It is important to note that the space between the calcite wedges should be minimized to eliminate any possible aberrations introduced on the converging beam, and that with a strongly converging beam any aberrations would be larger in magnitude. We leave a detailed analysis of such aberrations to a future work. In the following section we demonstrate our TWINS-INSIGHT device to characterize an ultrafast laser beam spatio-spectrally.

3. Spatio-spectral characterization of a beam with no applied couplings

To do a succesful spatio-spectral measurement we first calibrate the spectrum reconstructed using our specific calcite prisms and compare to that measured using a simple fiber-coupled spectrometer, and find that $|\Delta n_g| = 0.171$ for our case. This is a 6 % difference from the expected value of 0.1817, but this can be easily explained by a very small difference in the absolute refractive index of either axis from the literature values. Because these prisms are manufactured from naturally occurring crystals, this is not unexpected. With the 5 degree wedge angle of the prisms and this calibrated group-index difference, a step of 20 μm is required to change the delay by 1 fs.

We measured the 24 fs UHI-100 beam, a 100 TW Titanium:Sapphire-based system with pulses centered on 800 nm wavelength and operating at 10 Hz, in a tight-focusing geometry ($f/\# \sim 5$). We characterized the beam with very high attenuation to avoid any optical damage, and relay-imaged the small focal spot at the experimental focal position to the TWINS-INSIGHT setup using a near-infrared microscope objective to avoid unintended chromatic aberration (not shown in Fig. 1). In the end, to match the numerical aperture of the microscope objective we aperture the 6.5 cm diameter UHI-100 beam to have a diameter of roughly 3 cm. We emphasize that this is not an intrinsic limitation of the technique, but only one of the specific setup used for this experiment. The resulting focal spot on the TWINS-INSIGHT cameras has a roughly 150 μm beam diameter. Due to this relatively loose focusing within the TWINS wedges, the aberrations from the calcite wedges were minimal. The measurements were done without any

OSA CONTINUUM

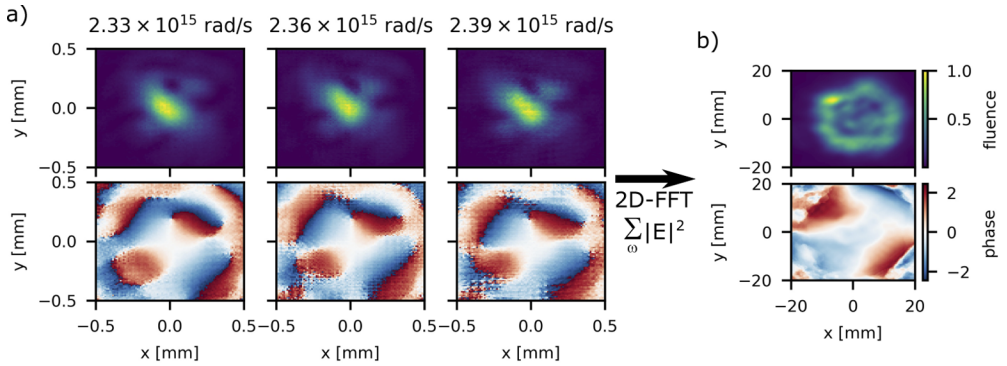

Fig. 2. Spatio-spectral measurement of the attenuated UHI-100 beam without any significant STCs. The far-field (a) is shown for three different frequencies left to right, with the amplitude shown on top and the spatial phase on the bottom. The far-field data is Fourier-transformed and scaled to calculate the amplitude and phase on the near-field collimated beam before focusing optics. The spectrally-integrated amplitude and spectrally-averaged spatial phase are shown in (b) on the top and bottom respectively, replicating standard beam profile and wavefront data. This data shows a clear achromatic astigmatism at 45 deg, responsible for the asymmetric focal spots in (a). The frequency-resolved data in (a) does not show any significant frequency-dependent aberrations in amplitude or phase.

averaging *at each delay* due to the relatively low repetition rate of the laser system. The results of the TWINS-INSIGHT measurement, with no applied STCs, are shown in Fig. 2.

The focal spots and spatial phase are shown for three different frequencies in Fig. 2(a), where there is clearly minimal variation between the different cases. This is consistent with the absence of significant STCs. However, it is clear that the focal spot nevertheless has achromatic aberrations. This suggests an achromatic wavefront aberration on the laser beam before focusing. We use the 2D spatial Fourier-transform to reconstruct the beam in the near-field before the focusing optics, shown in Fig. 2(b). We sum the intensity over all frequencies and normalize to the peak fluence, and we average the spatial phase weighted by the total energy at each frequency (i.e. a spectrally-weighted sum). This produces a reconstruction of the standard beamprofile and wavefront [17]. With these reconstructions in Fig. 2(b) we can see clear asymmetries on the collimated beam profile, and a clear astigmatism at 45 deg. in the wavefront. It is these achromatic imperfections that produce the aberrated focal spots in Fig. 2(a). Although we do not compare these results to a standard wavefront sensor, an astigmatism of this nature is common and not unexpected, and the INSIGHT technique has been validated in previous work [17]. This data is used as the reference data for the following section where we measure two main types of STC on the laser in the same conditions by adding a special afocal lens doublet, validating the suitability of the technique for measuring STCs.

4. Measurement of spatio-spectral couplings

As a proof-of-principle we measure common low-order STCs with the TWINS-INSIGHT device. We use a custom afocal doublet meant to impart a design value of pulse-front curvature (PFC) [18], previously characterized and confirmed to match the design value using an INSIGHT device with a Michelson interferometer [19]. The design of the doublet is detailed in the supplementary material of Ref. [18]. It consists of thick lenses of focal lengths 298 mm and -291 mm (at 800 nm wavelength) made from S-TIM-2 and PSK53A glasses respectively, separated by a distance of about 2 mm in order to essentially act as a telescope with unity magnification. The output beam has PFC but is collimated at the central frequency and roughly the same size as the input. In our

OSA CONTINUUM

case, Fig. 3(a), the lens with a negative focal length (the second lens) is composed of the glass with a higher group index than the first lens, producing a greater delay at the edges of the beam than at the center, and therefore a positive PFC α. The design value of PFC is 5.9 fs/cm^2.

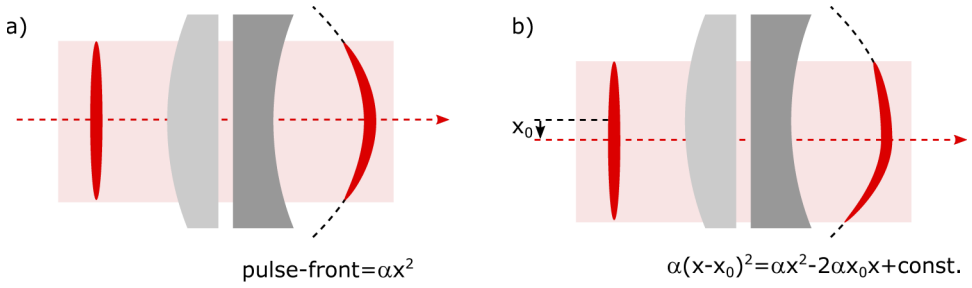

Fig. 3. A custom doublet composed of two singlet lenses with similar focal lengths but composed of different glasses. This doublet imparts only pulse-front curvature α on an ultrashort pulse (a) when the optical axis of the pulse and doublet overlap. If the pulse is off-center in one axis by an amount x_0 (b) the pulse-front has a combination of tilt ($-2\alpha x_0$) and curvature (still α).

Although this doublet is meant to impart PFC in optimum operation, it can also impart pulse-front tilt (PFT) when the optical axis of the doublet is offset transversely from the axis of the laser beam [20]. This concept is shown in Fig. 3. When the beam is centered on the doublet the spherical lenses composed of different glasses produce a radially-varying delay that is purely quadratic with a coefficient α corresponding to the magnitude of the PFC. If the doublet is not properly centered, Fig. 3(b), then the delay of the pulse-front is also no longer centered and no longer purely quadratic. The linear term in the pulse-front delay corresponds to a PFT in addition to the unchanged amount of PFC.

We measure again the broadband UHI-100 laser system with the doublet significantly off-center and compare to the case when the doublet has been better aligned. When analyzing the measurements we look primarily at the low-order Zernike coefficients for the spatial phase in the near-field beam *at each frequency* [3,4]. Specifically we analyze the wavefront curvature $(1/R)$ and the tilt in the x direction θ_x (corresponding to the horizontal axis in the lab coordinates) for each frequency, which are then related to the PFC and PFT in the x direction (η_x) as follows

$$\alpha = \frac{\omega_o}{2c}\frac{\partial\,(1/R)}{\partial\omega} \tag{2}$$

$$\eta_x = \frac{\omega_o}{c}\frac{\partial\theta_x}{\partial\omega}. \tag{3}$$

These relations are based on the time-frequency relation via the Fourier transform in ultrafast optics, and show the equivalence of PFC and PFT to chromatic phase aberrations. We also measure the tilt in the y direction θ_y (corresponding to the vertical axis in the lab coordinates), although it does not change. This allows us to confirm the vertical placement of the doublet as well.

The data is shown in Fig. 4, with the reference measurement with no doublet shown in panel (a), the measurement with the misaligned doublet in panels (b)–(c), and with the better aligned doublet in panels (d)–(f). The reference measurement is confirmed to have no significant PFC or PFT in either axis, indicated by the lack of a clear frequency dependence in Fig. 4(a) and as stipulated in the previous section. The case of the misaligned doublet in Fig. 4(b)–(c) shows the design value of PFC $\alpha = 5.9$ fs/cm^2 and a non-zero PFT $\eta_x = -6.3$ fs/cm. We translated the doublet horizontally to align it better to the center of the laser beam, with the results shown

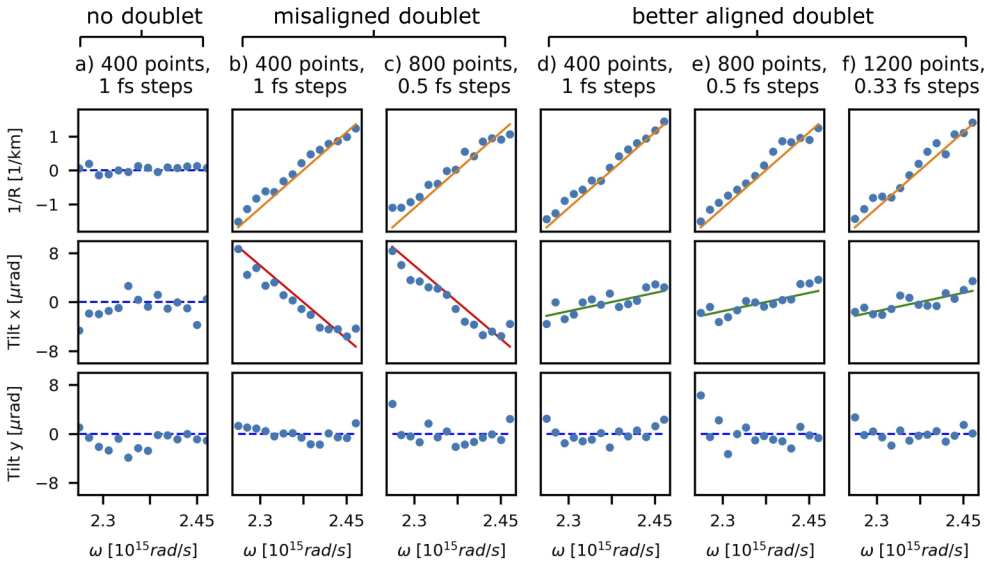

Fig. 4. Measurement with no doublet (a), with a misaligned doublet (b)–(c), and with a doublet that is better aligned (d)–(f) having various temporal delay steps, but a constant total delay range (i.e. constant frequency resolution). The top row shows the wavefront curvature, the middle row shows the tilt in the horizontal plane x, and the bottom row shows the tilt in the vertical plane y as a function of angular frequency. The orange lines in the top row of (b)–(f) correspond to the design PFC 5.9 fs/cm^2 of the doublet, the red lines in the middle row of (b)–(c) correspond to a PFT in x of -6.3 fs/cm, and the green lines in the middle row of (d)–(f) correspond to a reduced PFT in x of +1.6 fs/cm. The dashed blue lines in all other panels are a visual guide for a slope of zero.

in Fig. 4(d)–(f) where we measure the same PFC, but a PFT of smaller magnitude +1.6 fs/cm (-0.06 μrad/nm). According to our analysis this means that the doublet was initially misaligned by 5.3 mm and that we moved it by 6.7 mm towards the center of the laser beam such that it was finally 1.4 mm off-center in the other direction. Note that in all cases θ_y is essentially zero, confirming that the doublet was initially well aligned in the vertical direction and was thereafter translated only in the horizontal direction. Although the effects of such a doublet including misalignment are discussed recently in Ref. [20], we present here the first, to our knowledge, measurement of simultaneously controlled PFT and PFC with a very high accuracy (measuring below 0.1 μrad/nm in tilt variation).

The main measurements of the reference beam and the doublet were done with a delay step size of 1 fs, but we repeated measurements of the doublet with a 0.5 fs step size (Fig. 4(c) and (e)) and a 0.33 fs step size (Fig. 4(f)). Such a low step size extends the accessible spectral region deep in to the visible and is in general not possible with good stability when using piezo-electric stages. This is seen clearly in Fig. 5 for those three cases, where the accessible wavelength reaches 200 nm when using 0.33 fs steps. Although it was not necessary for our application since the spectrum remained centered on 800 nm, these results show that spatio-spectral measurements are possible using a birefringent delay line with such small step sizes. A 0.33 fs delay would require 50 nm steps with a piezo-electric stage, but required steps of 6.67 μm in our case—easily achievable and repeatable with high accuracy by the stick-slip stages used in the setup [21].

We would expect that the quality of the interferometry data would be comparable to previous TWINS measurements, and that as a result the STC data would be of better quality with the TWINS setup than with a Michelson interferometer. However, this turns out not to be the case,

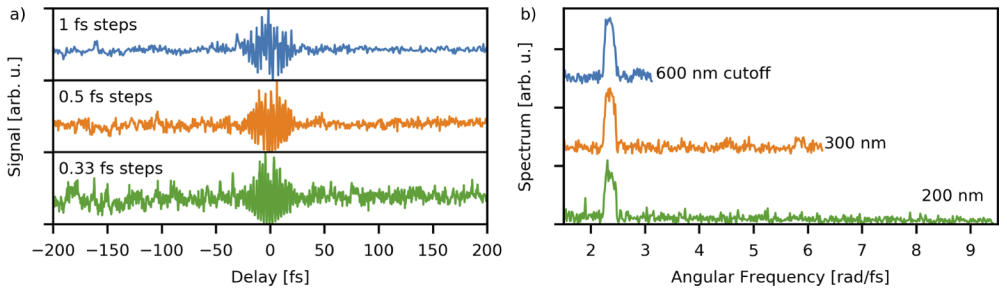

Fig. 5. Measurements with different step sizes. In panel (a) the interferences at only the central pixel on the beam profile are shown for three scans with the better aligned doublet having the same range of delays, but increasingly smaller steps (the same scans as for Fig. 4(d)–(f)). Each interferogram is normalized within its own panel such that the high fringe contrast where the pulse copies are interfering (between -25 fs and +25 fs delay) is clearly visible. The reconstructed spectra in panel (b) show clearly how the cutoff wavelength decreases (cutoff frequency increases), reaching 200 nm for the scan with 0.33 fs steps.

as the retrieved STC data in Fig. 4 are of comparable quality to previous measurements of such STCs using the INSIGHT device [4,19], and indeed, the raw interferograms in Fig. 5 are not of as good quality as those produced from the TWINS interferometer in past work. We attribute this observation to the fact that this is the first measurement of such a high-power and low rep-rate laser system using the TWINS interferometer and the first such measurement of any STCs. Past measurements with the TWINS device were, for example, spectroscopy with 1 kHz repetition rate lasers [6,22] or hyperspectral imaging of static environments [10,11]. The impact of the lack of averaging in the interferograms in Fig. 5 and the inherent instabilities in the laser system output (spectrum, wavefront, and even STCs) is not known specifically at this time and likely plays a large role. However, as seen in Fig. 5(b) and Fig. 4, both the spectrum and STCs can be measured despite the high noise level in the interferograms. Future work could assess the true benefits and limits of this technique for spatio-spectral characterization when applied to such highly complex and relatively low rep-rate laser systems, and especially when applied at much shorter wavelengths.

5. Conclusion

We have described the TWINS-INSIGHT device, a combination of the INSIGHT technique for spatio-spectral metrology of ultrashort pulses around the focus and the TWINS technique for doing spectroscopy with a birefringent delay line. Our device used calcite wedges, standard translation stages, and commonly available polarization optics to do spatio-spectral metrology of near-infrared 24 fs pulses from a 100 TW laser system operating at 10 Hz with pulse-front tilt and pulse-front curvature. With the addition of a measurement of the spectral phase at a single position the complex 3D field in time can be calculated and propagated to an arbitrary plane outside of focus. We tested with step sizes as low as 0.33 fs, much smaller than necessary for our specific application, but which can be necessary for more demanding applications such as measurement at shorter wavelengths. We believe that the TWINS-INSIGHT device could allow for highly stable spatio-spectral characterization of laser pulses with broad spectra going deep in the visible range, and allow for high precision delay steps and therefore low noise spectral reconstruction. Future work could assess the quality and limitations of the high precision and low noise goal, especially when applied to such high-power laser systems, and potentially show additional simplicity, speed, and functionality for certain applications by utilizing compressed sensing algorithms.

Funding. Horizon 2020 Framework Programme (CREMLINplus grant agreement no. 871072, ExCoMet ERC grant agreement no. 694596, LASERLAB grant agreement no. 871124); Laboratoire d'excellence Physique Atomes Lumière Matière (ANR-10-LABX-0039-PALM, project EXYT); Commissariat à l'Énergie Atomique et aux Énergies Alternatives (DRF Impulsion).

Acknowledgments. The authors would like to thank Fabrice Reau for operating the laser system and Ludovic Chopineau for help with the experimental setup. We acknowledge Antonin Borot and François Sylla for helpful discussions regarding the TWINS concept.

Disclosures. The authors declare no conflicts of interest.

Data availability. Data underlying the results presented in this paper are not publicly available at this time but may be obtained from the authors upon reasonable request.

References

1. S. Akturk, X. Gu, P. Bowlan, and R. Trebino, "Spatio-temporal couplings in ultrashort laser pulses," J. Opt. **12**(9), 093001 (2010).
2. C. Dorrer, "Spatiotemporal metrology of broadband optical pulses," IEEE J. Sel. Top. Quantum Electron. **25**(4), 1–16 (2019).
3. S. W. Jolly, O. Gobert, and F. Quéré, "Spatio-temporal characterization of ultrashort laser beams: a tutorial," J. Opt. **22**(10), 103501 (2020).
4. A. Borot and F. Quéré, "Spatio-spectral metrology at focus of ultrashort lasers: a phase-retrieval approach," Opt. Express **26**(20), 26444–26461 (2018).
5. A. R. Harvey and D. W. Fletcher-Holmes, "Birefringent fourier-transform imaging spectrometer," Opt. Express **12**(22), 5368–5374 (2004).
6. D. Brida, C. Manzoni, and G. Cerullo, "Phase-locked pulses for two-dimensional spectroscopy by a birefringent delay line," Opt. Lett. **37**(15), 3027–3029 (2012).
7. J. Réhault, M. Maiuri, C. Manzoni, D. Brida, J. Helbing, and G. Cerullo, "2D IR spectroscopy with phase-locked pulse pairs from a birefringent delay line," Opt. Express **22**(8), 9063–9072 (2014).
8. C. A. Manzoni, D. Brida, and G. N. F. Cerullo, "Phase-locked delay device including an optical wedge pair," (2015). US Patent 9, 182, 284.
9. A. Oriana, J. Réhault, F. Preda, D. Polli, and G. Cerullo, "Scanning fourier transform spectrometer in the visible range based on birefringent wedges," J. Opt. Soc. Am. A **33**(7), 1415–1420 (2016).
10. A. Perri, B. E. N. de Faria, D. C. T. Ferreira, D. Comelli, G. Valentini, F. Preda, D. Polli, A. M. de Paula, G. Cerullo, and C. Manzoni, "Hyperspectral imaging with a TWINS birefringent interferometer," Opt. Express **27**(11), 15956–15967 (2019).
11. A. Candeo, B. E. N. de Faria, M. Erreni, G. Valentini, A. Bassi, A. M. de Paula, G. Cerullo, and C. Manzoni, "A hyperspectral microscope based on an ultrastable common-path interferometer," APL Photonics **4**(12), 120802 (2019).
12. https://www.nireos.com/.
13. G. S. M. Jansen, D. Rudolf, L. Friesem, K. S. E. Eikema, and S. Witte, "Spatially resolved fourier transform spectroscopy in the extreme ultraviolet," Optica **3**(10), 1122–1125 (2016).
14. J. L. Ellis, K. M. Dorney, D. D. Hickstein, N. J. Brooks, C. Gentry, C. Hernández-García, D. Zusin, J. M. Shaw, Q. L. Nguyen, C. A. Mancuso, G. S. M. Jansen, S. Witte, H. C. Kapteyn, and M. M. Murnane, "High harmonics with spatially varying ellipticity," Optica **5**(4), 479–485 (2018).
15. C. Dorrer, N. Belabas, J.-P. Likforman, and M. Joffre, "Spectral resolution and sampling issues in fourier-transform spectral interferometry," J. Opt. Soc. Am. B **17**(10), 1795–1802 (2000).
16. M. Polyanskiy, "Refractive index database," https://refractiveindex.info/.
17. A. Jeandet, A. Borot, K. Nakamura, S. W. Jolly, A. J. Gonsalves, C. Tóth, H.-S. Mao, W. P. Leemans, and F. Quéré, "Spatio-temporal structure of a petawatt femtosecond laser beam," JPhys Photonics **1**(3), 035001 (2019).
18. A. Sainte-Marie, O. Gobert, and F. Quéré, "Controlling the velocity of ultrashort light pulses in vacuum through spatio-temporal couplings," Optica **4**(10), 1298–1304 (2017).
19. S. W. Jolly, O. Gobert, A. Jeandet, and F. Quéré, "Controlling the velocity of a femtosecond laser pulse using refractive lenses," Opt. Express **28**(4), 4888–4897 (2020).
20. A. Kabacinski, K. Oubrerie, J.-P. Goddet, J. Gautier, F. Tissandier, O. Kononenko, A. Tafzi, A. Leblanc, S. Sebban, and C. Thaury, "Measurement and control of main spatio-temporal couplings in a CPA laser chain," J. Opt. **23**(6), 06LT01 (2021).
21. https://www.smaract.com/linear-stages.
22. J. Réhault, R. Borrego-Varillas, A. Oriana, C. Manzoni, C. P. Hauri, J. Helbing, and G. Cerullo, "Fourier transform spectroscopy in the vibrational fingerprint region with a birefringent interferometer," Opt. Express **25**(4), 4403–4412 (2017).